Fibroblast Growth Factor 21 Regulates Lipolysis in White Adipose Tissue But Is Not Required for Ketogenesis and Triglyceride Clearance in Liver

Yuhei Hotta,* Hirotoshi Nakamura,* Morichika Konishi, Yusuke Murata, Hiroyuki Takagi, Shigenobu Matsumura, Kazuo Inoue, Tohru Fushiki, and Nobuyuki Itoh

Department of Genetic Biochemistry (Y.H., H.N., M.K., Y.M., H.T., N.I.), Kyoto University Graduate School of Pharmaceutical Sciences, Sakyo, Kyoto 606-8501, Japan; and Laboratory of Nutrition Chemistry (S.M., K.I., T.F.), Division of Food Science and Biotechnology, Graduate School of Agriculture, Kyoto University, Sakyo, Kyoto 606-8502, Japan

Fibroblast growth factors (Fgfs) are polypeptide growth factors with diverse functions. Fgf21, a unique member of the Fgf family, is expected to function as a metabolic regulator in an endocrine manner. Hepatic *Fgf21* expression was increased by fasting. The phenotypes of hepatic *Fgf21* transgenic or knockdown mice and high-fat, low-carbohydrate ketogenic diet-fed mice suggests that Fgf21 stimulates lipolysis in the white adipose tissue during normal feeding and is required for ketogenesis and triglyceride clearance in the liver during fasting. However, the physiological roles of Fgf21 remain unclear. To elucidate the physiological roles of Fgf21, we generated *Fgf21* knockout (KO) mice by targeted disruption. *Fgf21* KO mice were viable, fertile, and seemingly normal. Food intake, oxygen consumption, and energy expenditure were also essentially unchanged in *Fgf21* KO mice. However, hypertrophy of adipocytes, decreased lipolysis in adipocytes, and decreased blood nonesterified fatty acid levels were observed when *Fgf21* KO mice were fed normally. In contrast, increased lipolysis in adipocytes and increased blood nonesterified fatty acid levels were observed in *Fgf21* KO mice by fasting for 24 h, indicating that Fgf21 stimulates lipolysis in the white adipose tissue during feeding but inhibits it during fasting. In contrast, unexpectedly, hepatic triglyceride levels were essentially unchanged in *Fgf21* KO mice. In addition, ketogenesis in *Fgf21* KO mice was not impaired by fasting for 24 h. The present results indicate that Fgf21 regulates lipolysis in adipocytes in response to the metabolic state but is not required for ketogenesis and triglyceride clearance in the liver. **(*Endocrinology* 150: 4625–4633, 2009)**

Fibroblast growth factors (Fgfs) are polypeptide growth factors with diverse functions. *Fgf*s widely expressed in developing and adult tissues play important roles in development and metabolism. The human/mouse *Fgf* family comprises 22 members. Most Fgfs bind to and activate Fgf receptors on the cell surface, resulting in the activation of several cytoplasmic signal transduction pathways. They function in a paracrine or endocrine manner (1–3).

Although *Fgf21* was originally identified in mouse embryos, it is predominantly expressed in the liver among major adult tissues (4). Fgf21 is a member of the Fgf19/21/23 subfamily (3). Although most Fgfs act as growth or differentiation factors in a paracrine manner, Fgf19, Fgf21, and Fgf23 potentially function as metabolic regulators in an endocrine manner. Fgf19 and Fgf23 act to regulate bile acid and phosphate metabolism, respectively (5, 6).

Mammals have evolved complex metabolic responses to fasting. During fasting, nonesterified fatty acids (NEFAs) are released from the white adipose tissue (WAT) to the liver and

ISSN Print 0013-7227 ISSN Online 1945-7170
Printed in U.S.A.

doi: 10.1210/en.2009-0119 Received January 30, 2009. Accepted June 29, 2009.
First Published Online July 9, 2009

* Y.H. and H.N. contributed equally to this work.

Abbreviations: ES, Embryonic stem; Fgf, fibroblast growth factor; KD, ketogenic diet; KO, knockout; NEFA, nonesterified fatty acid; Ppar, peroxisome proliferator-activated receptor; RT-qPCR, RT-quantitative PCR; WAT, white adipose tissue.

oxidated to acetyl-CoA. From acetyl-CoA, hepatocytes synthesize ketone bodies, which become the predominant energy source for the brain (7). Peroxisome proliferator-activated receptor (Ppar)-α, a nuclear receptor activated by NEFAs, is a factor crucial for the normal adaptive response to fasting. Ketogenesis in the liver during fasting is greatly impaired in *Ppar*α knockout (KO) mice (8, 9). Hepatic *Fgf21* expression is induced directly by PPARα in response to fasting. The phenotypes of *Fgf21* transgenic mice indicate that Fgf21 stimulates lipolysis in the WAT and ketogenesis in the liver (10). The expression of *Fgf21* is also induced in the liver by a high-fat, low-carbohydrate ketogenic diet (KD) (11). In addition, adenoviral knockdown of hepatic *Fgf21* in KD-fed mice causes reduced levels of ketones in blood (11). Hepatic triglyceride levels are also significantly decreased in *Fgf21* transgenic mice (10). Adenoviral knockdown of hepatic *Fgf21* in KD-fed mice causes fatty liver and lipemia (11). These findings suggest that Fgf21 acts as a metabolic regulator that regulates lipolysis in the WAT and is required for ketogenesis and triglyceride clearance in the liver. However, the physiological roles of Fgf21 remain unclear.

To elucidate the physiological roles of Fgf21, we analyzed *Fgf21* KO mice generated by targeted disruption. The phenotypes of these mice also indicate that Fgf21 regulates lipolysis in adipocytes in response to metabolic state. Although hepatic *Fgf21* expression was greatly induced in response to fasting, the phenotypes of *Fgf21* KO mice clearly indicate that Fgf21 is not required for ketogenesis and triglyceride clearance in the liver.

Materials and Methods

Animal experiments

All mice were maintained in a light-controlled room (lights on from 0800 to 2000 h) and allowed free access to normal diet (MF; 3.6 kcal/g, 12% kcal fat, source: soybean; Oriental Yeast, Tokyo, Japan), except for fasting experiments. The experiments were performed using male mice. All mice at 2 months of age were acclimatized to housing for more than 5 d before experimentation. For the fasting experiments, mice were deprived of food for 24 h (from 1200 h). All mice were killed to obtain tissues and blood samples at 1200 h.

Expression analysis

Total RNA was extracted from mouse tissues using an RNeasy minikit (QIAGEN, Valencia, CA). cDNA was synthesized from the RNA (1 μg) as a template in a reaction mixture containing Moloney murine leukemia virus reverse transcriptase (Life Technologies, Inc., Lake Placid, NY) and a random hexadeoxynucleotide primer (Takara, Shiga, Japan). The cDNA was amplified by PCR with Taq DNA polymerase (Wako, Tokyo, Japan) and primers specific for *Fgf21*.

Gene targeting

Mouse *Fgf21* gene fragments, a 2.4-kb fragment for the 5′ homology recombination arm and a 7.4-kb fragment for the 3′ homology recombination arm, were amplified from the genomic DNA of 129 mouse embryonic stem (ES) cells as a template by PCR with KOD$^+$ DNA polymerase (TOYOBO, Osaka, Japan). A targeting vector was constructed by ligation of the fragments, the 5′ and 3′ homology recombination arms and a 6.3-kb fragment for an IRES-LacZ-polyA/PGK-neo cassette. A diphtheria toxin A expression cassette was inserted at the 5′ end of the targeting vector (12, 13). The coding region of mouse *Fgf21* is divided into three exons, exons 1–3. Most of exon 1 and all of exons 2 and 3 of *Fgf21* were replaced with the IRES-LacZ-polyA/PGK-neo cassette. Because most of the coding region (606 of 630 bases) of *Fgf21* was deleted, the mutant allele is likely to be null. The targeting vector was linearized with *Not*I and electroporated into C57BL/6 ES cells. The selection in G418 produced one homologous recombinant ES cell clone that was confirmed by Southern blot analysis using a 5′ probe. Mouse Fgf21 is located on chromosome 7. Germ-line chimeras were produced by the simple aggregation method (14) with *Fgf21*-disrupted ES (+/−) cells and morulae isolated from 129 Sv mice. Male chimeras were mated with C57BL/6 females to obtain F_1 *Fgf21*$^{+/-}$ mice. *Fgf21*$^{+/-}$ mice were maintained on a C57BL/6 background. Male and female *Fgf21*$^{+/-}$ mice were intercrossed to obtain wild-type and *Fgf21* KO littermates. Wild-type and *Fgf21* KO littermates from generation F3 to F7 were used for all experiments.

Genotyping of mice

Genotypes of mice were determined by PCR using the following primers: P1 (5′-GAC TGT TCA GTC AGG GAT TG-3′), P2 (5′-CCC GTG ATA TTG CTG AAG AG-3′), and P3 (5′-ACA GGG TCT CAG GTT CAA AG-3′). P1 and P3 produced a 541-bp fragment of the wild-type *Fgf21* locus. P2 and P3 produced a 243-bp fragment of a mutant *Fgf21* locus.

Histological analysis

The sc WAT of wild-type mice and *Fgf21* KO mice at 2 months of age was fixed in Bouin's fixative, dehydrated, embedded in paraffin, and sectioned. Sections (6 μm) were stained with hematoxylin and eosin and examined by light microscopy. Images of adipose tissue sections were captured and adipocyte sizes were measured for at least 300 cells per mice with Image J software (National Institutes of Health, Bethesda, MD). Unfixed livers of wild-type mice and *Fgf21* KO mice at 2 months of age were frozen in optimum cutting temperature compound. Frozen sections (16 μm) were stained with hematoxylin and eosin. Lipid droplets were revealed by staining with oil red O. Frozen sections were incubated with oil red O for 20 min at room temperature. After being washed with 60% isopropanol, livers were counterstained with hematoxylin.

Lipolytic activity

The sc WAT of wild-type mice and *Fgf21* KO mice at 2 months of age was homogenized in homogenizing buffer (50 mM Tris, 0.25 M sucrose, 1 mM EDTA, 20 μg/ml leupeptin, 2 μg/ml pepstatin). Cell debris was removed by centrifugation at 1000 $\times$ *g* for 15 min to obtain cell extracts. Protein concentration in cell extracts was determined by a Bio-Rad protein assay kit (Bio-Rad Laboratories, Hercules, CA) with BSA as the standard. Lipolytic

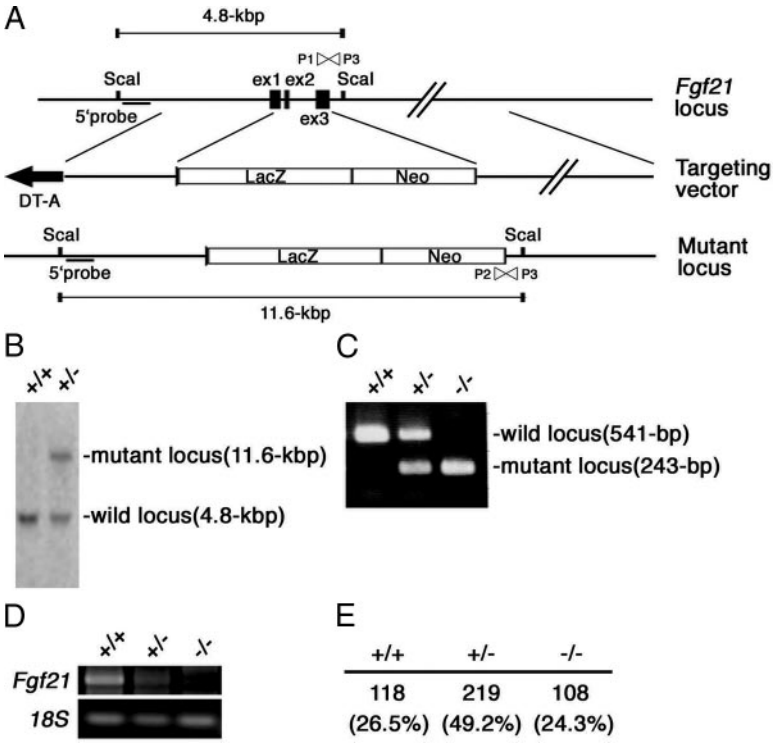

FIG. 1. Targeted disruption of *Fgf21* in mice. A, A targeting vector was constructed by ligation of three fragments, 5′ and 3′ homology recombination arms and a fragment for an IRES-LacZ-polyA/PGK-neo cassette. The coding region of mouse *Fgf21* is divided into three exons, exons 1–3. Most of exon 1 and all of exons 2 and 3 of *Fgf21* were replaced with the IRES-LacZ-polyA/PGK-neo cassette. The linearized targeting vector was electroporated into C57BL/6 ES cells. B, Wild-type (+/+) and *Fgf21*-disrupted (+/−) ES cells were examined by Southern blot analysis using a 5′ probe. The 4.8-kb and 11.6-kb fragments, which correspond to the wild-type and mutant loci, respectively, were detected from the genomic DNA digested with *Sca*I. C, Genotypes of wild-type (+/+), *Fgf21* heterozygous (+/−), and *Fgf21* knockout (−/−) mice were determined by PCR using the three primers, P1, P2, and P3 [wild (541 bp, P1/P3) and mutant (243 bp, P1/P2) loci]. D, *Fgf21* expression in the wild-type (+/+), *Fgf21* heterozygous (+/−), or *Fgf21* knockout (−/−) liver at 2 months of age was examined by RT-PCR using primers specific for exons 1 and 3. E, Mating of heterozygous mice resulted in offspring of three genotypes ($Fgf21^{+/+}$, $Fgf21^{+/-}$, and $Fgf21^{-/-}$) at normal Mendelian ratios.

activity in cell extracts was determined using *p*-nitrophenyl laurate as the substrate (15).

RT-quantitative PCR (RT-qPCR) analysis

Total RNA was prepared from tissues of wild-type mice and *Fgf21* KO mice at 2 months of age using an RNeasy mini kit (QIAGEN). cDNA was synthesized as described above. RT-qPCR was performed on a Thermal Cycler Dice (Takara), using SYBR Premix Ex Taq 2 (Takara). *18S* rRNA levels were used as an internal control.

Blood parameter analysis

Blood samples were obtained from wild-type and *Fgf21* KO mice at 2 months of age. Blood glucose levels were measured by a Glutest R kit (Sanwa Kagaku, Nagoya, Japan). Plasma triglyceride, NEFAs, and β-hydroxybutyrate levels were measured using triglyceride E-Test (Wako), NEFA C-Test (Wako), and ketone test B (Sanwa Kagaku) kits, respectively. Plasma insulin and glucagon levels were measured using mouse insulin ELISA (Morinaga, Tokyo, Japan) and glucagon ELISA (Wako) kits, respectively.

Hepatic parameter analysis

Hepatic triglyceride and glycogen levels in wild-type and *Fgf21* KO mice at 2 months of age were measured using triglyceride E-Test (Wako) and glycogen assay (BioVision, Mountain View, CA) kits, respectively.

Measurement of oxygen consumption

Oxygen consumption of normal-feeding wild-type and *Fgf21* knockout mice was measured with an indirect calorimetric system. In brief, room air was pumped through an acrylic metabolic chamber, and the expired gas was filtered through thin cotton, dried, and subjected to gas analysis (model RL-600; Alco System, Tokyo, Japan). In addition, energy expenditure was calculated as the product of the calorific value of oxygen [$3.815 + (1.232 \times$ respiratory quotient)] and the volume of O_2 consumed.

Statistical analysis

Data are expressed as means ± SEM. The statistical significance of differences in mean values was assessed with Student's *t* test or Welch's *t* test. $P < 0.05$ was considered statistically significant.

Results

Targeted disruption of *Fgf21*

Fgf21 is expected to play roles in lipid metabolism from the phenotypes of hepatic *Fgf21* transgenic or knockdown mice (10, 11, 16). To address the physiological roles of *Fgf21* in mice, we generated *Fgf21* KO mice by targeted disruption (Fig. 1A). A targeted ES cell clone was identified by Southern blot hybridization analysis using a 5′ probe (Fig. 1, A and B). Mice bearing the targeted allele were generated by standard procedures. Genotyping of mice was confirmed by PCR using primers specific for the wild-type and mutant loci (Fig. 1C). In addition, *Fgf21* expression in the liver at 2 months of age was also examined by RT-PCR using primers specific for exon 1 and exon 3. *Fgf21* expression was detected in the wild-type and heterozygous liver but not *Fgf21* KO liver (Fig. 1D). Mating of heterozygous mice resulted in offspring of three genotypes ($Fgf21^{+/+}$, $Fgf21^{+/-}$, and $Fgf21^{-/-}$) at normal Mendelian ratios (Fig. 1E). *Fgf21* KO mice were viable at least until 14 months of age and fertile (data not shown).

Fgf21 KO mice at 2 months of age were seemingly normal (Fig. 2A), and their body and tibia lengths were essentially unchanged (Fig. 2, C and D). We also examined the body weights of normal-feeding wild-type and *Fgf21*

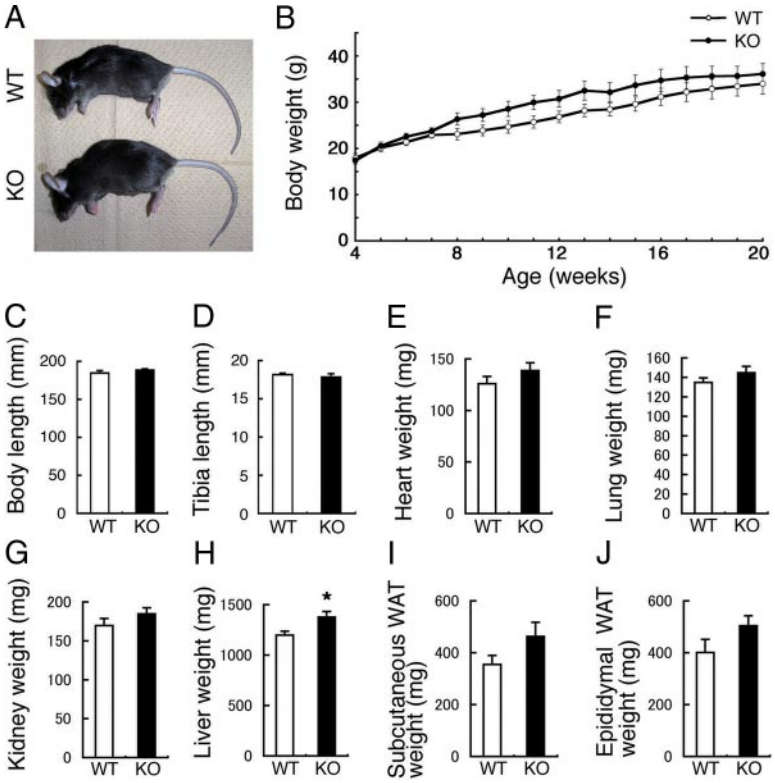

FIG. 2. Body and tissue weights of wild-type and *Fgf21* KO mice. A, Appearances of wild-type (WT) and *Fgf21* KO mice at 2 months of age are shown. B, Body weight gain of wild-type and *Fgf21* KO mice from 4 to 20 wk of age. All mice were weighed weekly (n = 7 mice per group). C, Body lengths of wild-type (WT) and *Fgf21* KO mice at 2 months of age are shown (n = 3 mice per group). In this and all other figures, *error bars* represent the mean ± SEM. D, Tibia lengths of wild-type (WT) and *Fgf21* KO mice at 2 months of age are shown (n = 3 mice per group). E–J, The heart, lung, kidney, liver, epididymal WAT, and inguinal sc WAT weights of wild-type and *Fgf21* KO mice at 2 months of age (n = 9–11 mice per group). *, $P < 0.05$ *vs.* wild-type mice.

KO males from 4 to 20 wk of age (Fig. 2B). The body weights of *Fgf21* KO mice at 4 wk of age were essentially unchanged. However, the *Fgf21* KO mice were slightly heavier than the wild-type mice from 8 wk of age. Food intake and the diurnal variation (dark/light) in food intake were essentially indistinguishable between the two groups (Fig. 3A). In addition, oxygen consumption and energy expenditure were essentially indistinguishable between the two groups (Fig. 3, B–D). We also examined the weights of the heart, liver, lung, kidney, inguinal sc WAT, and epididymal WAT of *Fgf21* KO mice at 2 months of age. The weights of the heart, lung, and kidney were essentially unchanged (Fig. 2, E–G). In contrast, the weight of the liver was slightly increased ($P < 0.05$) (Fig. 2H). In addition, the weights of the sc and epididymal WATs were increased ($P = 0.13$ and 0.11), respectively (Fig. 2, I and J).

Lipolysis in WAT of normal-feeding *Fgf21* KO mice

The sc and epididymal WAT weights of normal-feeding *Fgf21* KO mice at 2 months of age were increased as described above. In addition, because the mature adipocytes in the WATs of *Fgf21* transgenic mice were decreased in size (10, 17), we examined the sizes of mature adipocytes in normal-feeding *Fgf21* KO mice. The mature adipocytes in the sc WAT were larger in the *Fgf21* KO mice than wild-type mice ($P = 0.08$) (Fig. 4, A and C). The mature adipocytes in the epididymal WAT of *Fgf21* KO mice also were larger (data not shown).

Fgf21 protein stimulated lipolysis in cultured adipocytes (10). Therefore, lipolytic activity in the WAT of normal-feeding *Fgf21* KO mice was examined. Lipolytic activity was decreased ($P = 0.06$) (Fig. 4D). The expression of *hormone-sensitive lipase* (*Hsl*) and *adipose triglyceride lipase* (*Atgl*), the predominant lipase genes in the WAT, was significantly increased in the WAT of *Fgf21* transgenic mice (10). Therefore, we also examined the expression of *Hsl* and *Atgl* in the sc WAT of normal-feeding *Fgf21* KO mice at 2 months of age by RT-qPCR (Fig. 4, E and F). Their expression was significantly decreased ($P < 0.05$). These results indicate that Fgf21 stimulates lipolysis in the WAT during normal feeding.

Blood parameters in normal-feeding *Fgf21* KO mice

Increased blood NEFA levels and decreased blood triglyceride levels were observed in *Fgf21* transgenic mice (10). In addition, the phenotypes of *Fgf21* KO mice indicate that Fgf21 stimulates lipolysis in the WAT as described above. Therefore, we examined blood glucose, NEFA, and triglyceride levels in normal-feeding *Fgf21* KO mice at 2 months of age (Fig. 5, A–C). Glucose and triglyceride levels were essentially unchanged. In contrast, NEFA levels were decreased of wild-type mice ($P = 0.13$). These results indicate that Fgf21 regulates NEFA metabolism but not glucose and triglyceride metabolism. Because insulin and glucagon regulate energy homeostasis, we examined blood insulin and glucagon levels in normal-feeding *Fgf21* KO mice. Insulin and glucagon levels were essentially unchanged (Fig. 5, E and F).

Ketogenesis in fasted *Fgf21* KO mice

Hepatic *Fgf21* expression and blood ketone, β-hydroxybutyrate, levels were markedly increased by fasting in wild-type mice (10, 11). In addition, blood β-hydroxybutyrate levels were increased in *Fgf21* transgenic mice. Therefore, it was proposed that Fgf21 is essential for ketogenesis in the liver during fasting (10, 11). To examine the possible

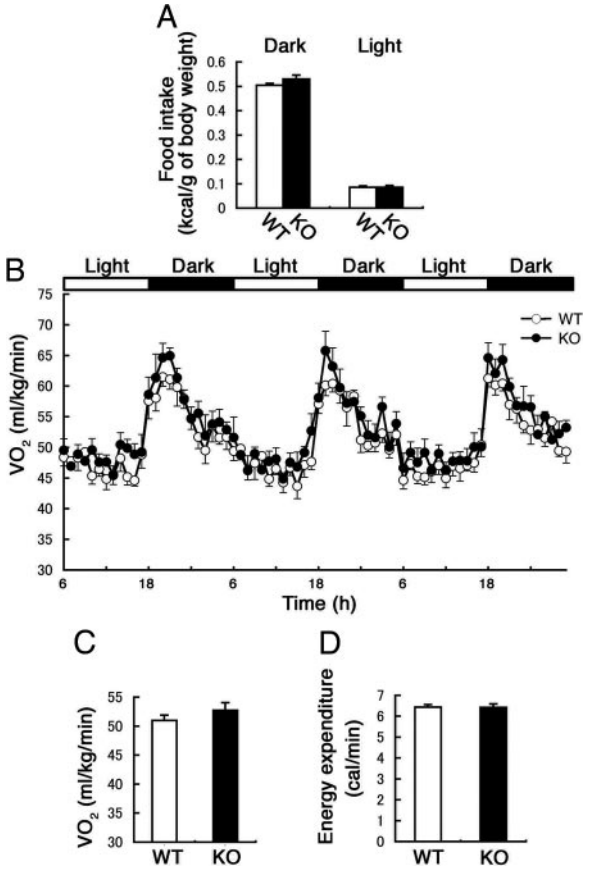

FIG. 3. Food intake, and metabolic rate of wild-type and *Fgf21* KO mice. A, The food intake and its diurnal variation (dark/light) in wild-type (WT) and *Fgf21* KO mice at 2 months of age are shown (n = 4–6 mice per group). B, Whole-body oxygen consumption rate (VO_2, expressed in milliliters per kilogram of body weight per minute) during three 12-h light, 12-h dark cycles in normal feeding wild-type (WT) and *Fgf21* KO mice at 2 months of age is shown (n = 6–7 mice per group). Dark, 1800 to 0600 h; light, 0600 to 1800 h. C, Average values of VO_2 for the 24-h period are shown (n = 6–7 mice per group). D, Average values of energy expenditure for the 24-h period in the experiments are shown (n = 6–7 mice per group).

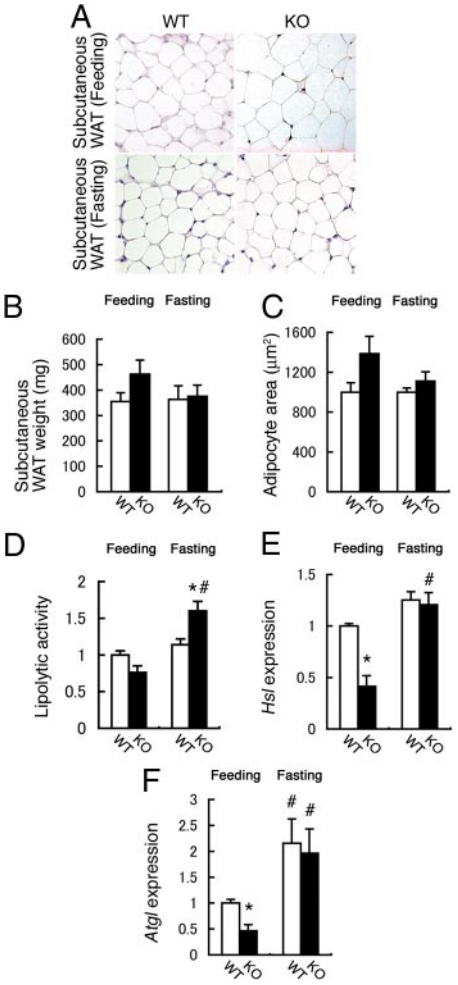

FIG. 4. Histological analysis, lipase gene expression, and lipolytic activity in sc WAT of wild-type and *Fgf21* KO mice. A, Paraffin sections of sc WAT of wild-type and *Fgf21* KO mice at 2 months of age were stained with hematoxylin and eosin. WT, Wild-type. *Scale bar*, 100 μm. B and C, Subcutaneous WAT weights and adipocyte cell areas of wild-type and *Fgf21* KO mice at 2 months of age during normal feeding and fasting. The average adipocyte cell areas were measured using at least 300 cells per mouse with Image J software (n = 5–11 mice per group). D, Lipolytic activity of the sc WAT of wild-type and *Fgf21* KO mice at 2 months of age during normal feeding and fasting was determined using *p*-nitrophenyl laurate as the substrate (n = 3–4 mice per group). *, $P < 0.05$ *vs.* wild-type mice within the same condition; #, $P < 0.05$ *vs.* feeding within the same genotype. E and F, The expressions of *Atgl* and *Hsl* in the sc WAT of wild-type and *Fgf21* KO mice at 2 months of age during normal feeding and fasting were determined by RT-qPCR (n = 3–9 mice per group). *, $P < 0.05$ *vs.* wild-type mice within the same condition; #, $P < 0.05$ *vs.* feeding within the same genotype.

role of Fgf21 in ketogenesis in the liver during fasting, we examined blood β-hydroxybutyrate levels in *Fgf21* KO mice fasted for 24 h. We confirmed that hepatic *Fgf21* expression and blood β-hydroxybutyrate levels were significantly increased in wild-type mice by fasting for 24 h ($P < 0.05$) (Figs. 6A and 5D). However, unexpectedly, blood β-hydroxybutyrate levels were also significantly increased in *Fgf21* KO mice by fasting ($P < 0.05$) (Fig. 5D). The β-hydroxybutyrate levels were significantly higher than those in wild-type mice ($P < 0.05$). These results clearly indicate that Fgf21 is not essential for ketogenesis in the liver during fasting.

Hepatic gene expression involved in ketogenesis in *Fgf21* KO mice

As described above, blood β-hydroxybutylate levels were markedly increased in *Fgf21* KO mice by fasting. Therefore, we examined the hepatic expression of genes involved in ketogenesis, including *Pparα*, *acyl-CoA oxidase* (*Acox1*) (18), *carnitine palmitoyltransferase 1a* (*Cpt1a*) (19), and *hydroxymethylglutalyl-CoA synthase 2* (*Hmgcs2*) (20) in *Fgf21* KO mice. The expression of all genes examined was significantly increased in wild-type mice by fasting for 24 h ($P < 0.05$) (Fig. 6, B–E); however, the expression was also significantly increased in the fasted *Fgf21* KO mice ($P < 0.05$). The expression levels in *Fgf21* KO mice were similar to those in wild-type mice

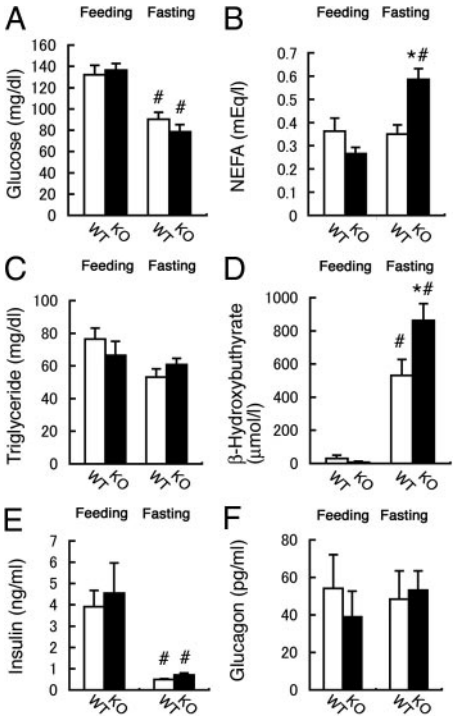

FIG. 5. Blood parameters in wild-type and *Fgf21* KO mice. A–F, Blood glucose, NEFA, triglyceride, β-hydroxybutyrate, insulin, and glucagon levels in wild-type and *Fgf21* KO mice at 2 months of age during normal feeding and fasting. WT, Wild-type (n = 5–12 mice per group). *, $P < 0.05$ *vs.* wild-type mice within the same condition; #, $P < 0.05$ *vs.* feeding within the same genotype.

(Fig. 6, B–E). These results also indicate that Fgf21 is not required for ketogenesis in the liver.

Hepatic lipid and glycogen levels in *Fgf21* KO mice

Hepatic triglyceride levels are significantly decreased in *Fgf21* transgenic mice (10). In contrast, hepatic triglyceride levels are significantly increased by knockdown of hepatic *Fgf21* in KD-fed mice (11). We also examined hepatic triglyceride levels in *Fgf21* KO mice at 2 months of age. Levels were essentially unchanged in normal-feeding *Fgf21* KO mice (Fig. 6F). In contrast, they were significantly increased in wild-type mice after fasting for 24 h ($P < 0.05$) (Fig. 6F); however, triglyceride levels were also significantly increased in fasted *Fgf21* KO mice to a similar extent ($P < 0.05$) (Fig. 6F). We examined *Fgf21* KO livers by histochemical means with hematoxylin and eosin staining and oil red O staining. *Fgf21* KO livers were apparently normal during both feeding and fasting (Fig. 6H). These results indicate that Fgf21 does not regulate triglyceride levels in the liver. Because liver weights were slightly increased in normal-feeding *Fgf21* KO mice at 2 months of age as described above (Fig. 2H), we also examined hepatic glycogen levels in *Fgf21* KO mice; however, glycogen levels in normal-feeding and fasted *Fgf21* KO mice were comparable with those in wild-type mice (Fig. 6G). These results indicate that the slightly increased liver weights are not due to hepatic triglyceride and glycogen levels. The mechanism of the slight increase remains to be elucidated.

Blood parameters and lipolysis in WAT of fasted *Fgf21* KO mice

As described above, Fgf21 plays crucial roles in NEFA metabolism in the WAT in normal-feeding mice. We also examined blood glucose and lipid levels and the subcutaneous WAT of *Fgf21* KO mice fasted for 24 h. The glucose levels in fasted wild-type and *Fgf21* KO mice were significantly decreased to a similar extent ($P < 0.05$) (Fig. 5A). In contrast, the NEFA levels, although essentially unchanged in the wild-type mice, were significantly increased in the *Fgf21* KO mice ($P < 0.05$), resulting that the NEFA levels in fasted *Fgf21* KO mice were significantly higher than those in wild-type mice ($P < 0.05$) (Fig. 5B). The triglyceride levels in fasted *Fgf21* KO mice were comparable with those in fasted wild-type mice (Fig. 5C). Insulin levels in fasted wild-type and *Fgf21* KO mice were significantly decreased to similar levels ($P < 0.05$) (Fig. 5E). In contrast, glucagon levels were essentially unchanged in both normal-feeding and fasted *Fgf21* KO mice (Fig. 5F). Although WAT weight was essentially unchanged in wild-type mice by fasting, it was decreased in *Fgf21* KO mice ($P = 0.25$) (Fig. 4B); the sizes of mature adipocytes were also decreased in *Fgf21* KO mice by fasting ($P = 0.41$) (Fig. 4, A and C). Lipolytic activity in the WAT was significantly increased in fasted *Fgf21* KO mice ($P < 0.05$), although its activity was essentially unchanged in fasted wild-type mice (Fig. 4D). The expression of *Hsl* and *Atgl* in the WAT was significantly increased to similar levels in fasted wild-type and *Fgf21* KO mice ($P < 0.05$) (Fig. 4, E an F). These results indicate that lipolysis in the WAT is significantly stimulated in *Fgf21* KO mice by fasting.

Discussion

Fgf21 is expected to be a metabolic regulator that acts in an endocrine manner (1, 16). Therapeutic administration of recombinant Fgf21 reduced blood glucose and triglyceride levels in diabetic mice. In addition, *Fgf21* transgenic mice exhibited a decrease in body weight and hypotrophy of mature adipocytes (17). Recently Inagaki *et al.* (10) also reported that *Fgf21* transgenic mice showed hypotrophy of adipocytes and enhanced lipolysis in adipocytes. Fgf21 protein stimulated lipolysis in cultured adipocytes (10). These results indicate potential roles of Fgf21 in lipolysis in the WAT.

Fgf21 KO mice feeding normally showed modest increase in body weight and hypertrophy of adipocytes in the WAT. These phenotypes are essentially consistent with

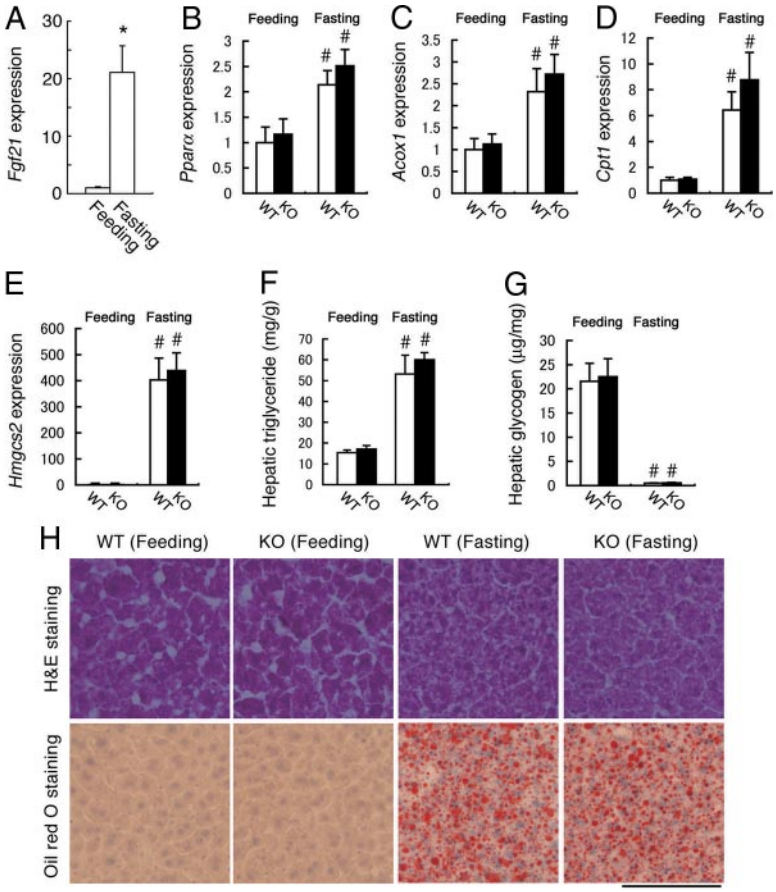

FIG. 6. Hepatic gene expression, triglyceride and glycogen levels, and histological analysis in wild-type and *Fgf21* KO mice. A, Hepatic *Fgf21* expression in wild-type mice during normal feeding and fasting was determined by RT-qPCR (n = 3–4 mice per group). *, $P < 0.05$ *vs.* feeding. B–E, Hepatic expression of genes involved in ketogenesis in wild-type and *Fgf21* KO mice during normal feeding and fasting was determined by RT-qPCR. WT, Wild-type (n = 5–9 mice per group). #, $P < 0.05$ *vs.* feeding within the same genotype. F and G, Hepatic triglyceride and glycogen levels in wild-type and *Fgf21* KO mice at 2 months of age during normal feeding and fasting (n = 5–9 mice per group). #, $P < 0.05$ *vs.* feeding within the same genotype. H, Frozen sections of the liver of wild-type and *Fgf21* KO mice at 2 months of age during normal feeding and fasting were stained with hematoxylin and eosin or oil red O. *Scale bar*, 100 μm.

that of *Fgf21* transgenic mice and that Fgf21 protein stimulates lipolysis in cultured adipocytes (10, 17). In addition, decreased blood NEFA levels, lipolytic activity, and *Hsl* and *Atgl* expression levels in *Fgf21* KO mice are essentially consistent with increased blood NEFA levels and *Hsl* and *Atgl* expression levels in *Fgf21* transgenic mice (10). The present results obtained using *Fgf21* KO mice support the proposal that Fgf21 stimulates lipolysis in the WAT (10, 17); however, blood insulin and glucagon levels were essentially unchanged in Fgf21 KO mice. These results indicate that insulin and glucagon levels play essentially no roles in decreased lipolysis in *Fgf21* KO mice.

Systemic administration of Fgf21 protein in obese mice lowers their mean body weight (21). Fgf21-treated mice exhibit increased energy expenditure, suggesting that hypertrophy of adipocytes in *Fgf21* KO mice might be caused in part by decreased energy expenditure; however, energy expenditure was essentially unchanged in *Fgf21* KO mice, indicating that adipocyte hypertrophy is not caused by energy expenditure.

Hepatic *Fgf21* expression is markedly induced by Pparα. The Pparα-Fgf21 signaling pathway was found to be essential for ketogenesis in the liver during fasting using *Fgf21* transgenic mice and hepatic *Fgf21* knockdown mice (10, 11). However, blood β-hydroxybutyrate levels were markedly increased in *Fgf21* KO mice by fasting. These results are inconsistent with those reported previously (10, 11). The present findings clearly demonstrate that Fgf21 is not required for ketogenesis. The phenotypes of *Fgf21* KO livers were mostly inconsistent with those of the *Fgf21* transgenic liver, indicating that most of the phenotypes of *Fgf21* transgenic livers might be due to pharmacological effects but not physiological effects of Fgf21. Blood β-hydroxybutyrate levels during fasting were significantly higher in *Fgf21* KO mice than wild-type mice. However, the hepatic expression of genes involved in ketogenesis was essentially unchanged in *Fgf21* KO mice. Infusion of exogenous NEFAs or induction of lipolysis can induce ketogenesis without changing the activity of the ketogenic enzymes (22, 23). As blood NEFA levels were significantly increased in *Fgf21* KO mice by fasting, the β-hydroxybutylate levels in fasted *Fgf21* KO mice might be partially due to NEFAs in blood.

Adenovirus-mediated hepatic *Fgf21* knockdown mice fed by a KD for 3 d resulted in gross changes in hepatic appearance by comparison with KD-fed wild-type mice. *Fgf21* knockdown livers became pale, friable, and fatty in nature and accumulated triglyceride (11). In addition, blood triglyceride levels were significantly increased in KD-fed *Fgf21* knockdown mice in comparison with KD-fed wild-type mice (11). We also examined *Fgf21* knockout mice fed KD for 6 d. Blood β-hydroxybutylate levels were significantly increased (more than 10-fold) in both KD-fed wild-type and *Fgf21* KO mice. Essentially no obvious changes in hepatic appearance and triglyceride levels were observed in KD-fed *Fgf21* knockout mice in comparison with KD-fed wild-type mice (our unpublished observations). In addition, the blood triglyceride levels in KD-fed *Fgf21* KO mice were not increased (our unpublished observations), indicating

that adenoviral knockdown might result in nonspecific effects in the liver.

Fgf15, Fgf21, and Fgf23 are members of the mouse Fgf15/21/23 subfamily (1). Because Fgfs within a subfamily have similar receptor-binding properties and overlapping patterns of expression, their functional redundancy is likely to occur (1). We also examined the expressions of *Fgf15* and *Fgf23* in wild-type and *Fgf21* KO livers by RT-PCR; however, their expressions were not detected by normal feeding and fasting for 24 h (our unpublished observations).

Hepatic *Fgf21* expression was greatly induced in response to fasting. In contrast to normal feeding, blood NEFA levels and lipolytic activity in fasted *Fgf21* KO mice were higher than in fasted wild-type mice, indicating that Fgf21 inhibited lipolysis in the WAT in fasted mice. These findings indicate that Fgf21 regulates lipolysis in adipocytes in response to the metabolic state. Although Fgf21 induced basal lipolysis in 3T3-L1 (10), Fgf21 attenuated hormone-stimulated lipolysis in human adipocytes (24). These *in vitro* experiments also support that Fgf21 regulates lipolysis in adipocytes in response to the metabolic state. However, *Atgl* and *Hsl* gene expression levels in fasted *Fgf21* KO mice was indistinguishable from those in fasted wild-type mice. Therefore, the mechanism of increase in lipolytic activity in fasted *Fgf21* KO mice remains to be elucidated.

Recently Izumiya *et al.* (25) reported that the expression of *Fgf21* was significantly induced in skeletal muscle of skeletal muscle-specific Akt1 transgenic mice. We also examined the expression of *Fgf21* in skeletal muscle of wild-type mice by RT-PCR. *Fgf21* expression could not be detected by normal feeding or fasting for 24 h (our unpublished observations), indicating that skeletal muscle is not a source of Fgf21 in wild-type mice both during normal feeding and fasting.

In conclusion, the present findings demonstrate that Fgf21 regulates lipolysis in the WAT. Fgf21 stimulates lipolysis in the WAT during normal feeding by regulating lipase gene expression but inhibits it during fasting. Blood NEFA levels are possibly regulated by lipolysis regulated by Fgf21. These results indicate that Fgf21 regulates lipolysis in adipocytes in response to the metabolic state. In contrast, Fgf21 is not required for ketogenesis and triglyceride clearance in the liver. The present findings will provide new insight into the molecular mechanism underlying lipid metabolism.

Acknowledgments

Address all correspondence and requests for reprints to: Morichika Konishi, Ph.D., Department of Genetic Biochemistry, Kyoto University Graduate School of Pharmaceutical Sciences, Sakyo, Kyoto 606-8501, Japan. E-mail: mkonishi@pharm.kyoto-u.ac.jp; or Nobuyuki Itoh, Ph.D., Department of Genetic Biochemistry, Kyoto University Graduate School of Pharmaceutical Sciences, Sakyo, Kyoto 606-8501, Japan. E-mail: itohnobu@pharm.kyoto-u.ac.jp.

This work was supported by the Ministry of Education, Science, Culture, Sports, and Technology, Japan (to M.K., N.I.); the Takeda Science Foundation (to N.I.); the Research Foundation for Pharmaceutical Sciences (to M.I.); and the Tokyo Biochemical Research Foundation (to M.K.).

Disclosure Summary: The authors have nothing to disclose.

References

1. **Itoh N, Ornitz DM** 2004 Evolution of the Fgf and Fgfr gene families. Trends Genet 20:563–569
2. **Thisse B, Thisse C** 2005 Functions and regulations of fibroblast growth factor signaling during embryonic development. Dev Biol 287:390–402
3. **Itoh N, Ornitz DM** 2008 Functional evolutionary history of the mouse Fgf gene family. Dev Dyn 237:18–27
4. **Nishimura T, Nakatake Y, Konishi M, Itoh N** 2000 Identification of a novel FGF, FGF-21, preferentially expressed in the liver. Biochim Biophys Acta 1492:203–206
5. **Yu X, White KE** 2005 FGF23 and disorders of phosphate homeostasis. Cytokine Growth Factor Rev 16:221–232
6. **Houten SM** 2006 Homing in on bile acid physiology. Cell Metab 4:423–424
7. **Cahill Jr GF** 2006 Fuel metabolism in starvation. Annu Rev Nutr 26:1–22
8. **Kersten S, Seydoux J, Peters JM, Gonzalez FJ, Desvergne B, Wahli W** 1999 Peroxisome proliferator-activated receptor alpha mediates the adaptive response to fasting. J Clin Invest 103:1489–1498
9. **Leone TC, Weinheimer CJ, Kelly DP** 1999 A critical role for the peroxisome proliferator-activated receptor α (PPARα) in the cellular fasting response: the PPARα-null mouse as a model of fatty acid oxidation disorders. Proc Natl Acad Sci USA 96:7473–7478
10. **Inagaki T, Dutchak P, Zhao G, Ding X, Gautron L, Parameswara V, Li Y, Goetz R, Mohammadi M, Esser V, Elmquist JK, Gerard RD, Burgess SC, Hammer RE, Mangelsdorf DJ, Kliewer SA** 2007 Endocrine regulation of the fasting response by PPARα-mediated induction of fibroblast growth factor 21. Cell Metab 5:415–425
11. **Badman MK, Pissios P, Kennedy AR, Koukos G, Flier JS, Maratos-Flier E** 2007 Hepatic fibroblast growth factor 21 is regulated by PPARα and is a key mediator of hepatic lipid metabolism in ketotic states. Cell Metab 5:426–437
12. **Ohbayashi N, Shibayama M, Kurotaki Y, Imanishi M, Fujimori T, Itoh N, Takada S** 2002 FGF18 is required for normal cell proliferation and differentiation during osteogenesis and chondrogenesis. Genes Dev 16:870–879
13. **Kassai Y, Munne P, Hotta Y, Penttilä E, Kavanagh K, Ohbayashi N, Takada S, Thesleff I, Jernvall J, Itoh N** 2005 Regulation of mammalian tooth cusp patterning by ectodin. Science 309:2067–2070
14. **Wood SA, Pascoe WS, Schmidt C, Kemler R, Evans MJ, Allen ND** 1993 Simple and efficient production of embryonic stem cell-embryo chimeras by coculture. Proc Natl Acad Sci USA 90:4582–4585
15. **Lehner R, Verger R** 1997 Purification and characterization of a porcine liver microsomal triacylglycerol hydrolase. Biochemistry 36:1861–1868
16. **Kharitonenkov A, Shanafelt AB** 2008 Fibroblast growth factor-21 as a therapeutic agent for metabolic diseases. Biodrugs 22:37–44
17. **Kharitonenkov A, Shiyanova TL, Koester A, Ford AM, Micanovic R, Galbreath EJ, Sandusky GE, Hammond LJ, Moyers JS, Owens RA, Gromada J, Brozinick JT, Hawkins ED, Wroblewski VJ, Li DS,**

Mehrbod F, Jaskunas SR, Shanafelt AB 2005 FGF21 as a novel metabolic regulator. J Clin Invest 115:1627–1635

18. **Aoyama T, Tsushima K, Souri M, Kamijo T, Suzuki Y, Shimozawa N, Orii T, Hashimoto T** 1994 Molecular cloning and functional expression of a human peroxisomal acyl-coenzyme A oxidase. Biochem Biophys Res Commun 198:1113–1118
19. **Britton CH, Mackey DW, Esser V, Foster DW, Burns DK, Yarnall DP, Froguel P, McGarry JD** 1997 Fine chromosome mapping of the genes for human liver and muscle carnitine palmitoyltransferase I (CPT1A and CPT1B). Genomics 40:209–211
20. **Quant PA, Tubbs PK, Brand MD** 1990 Glucagon activates mitochondrial 3-hydroxy-3-methylglutaryl-CoA synthase *in vivo* by decreasing the extent of succinylation of the enzyme. Eur J Biochem 187:169–174
21. **Coskun T, Bina HA, Schneider MA, Dunbar JD, Hu CC, Chen Y, Moller DE, Kharitonenkov A** 2008 FGF21 corrects obesity in mice. Endocrinology 149:6018–6027
22. **Bates MW, Linn LC, Huen AH** 1976 Effects of oleic acid infusion on plasma free fatty acids and blood ketone bodies in the fasting rat. Metabolism 25:361–373
23. **Avogaro A, Cryer PE, Bier DM** 1992 Epinephrine's ketogenic effect in humans is mediated principally by lipolysis. Am J Physiol 263: E250–E260
24. **Arner P, Pettersson A, Mitchell PJ, Dunbar JD, Kharitonenkov A, Rydén M** 2008 FGF21 attenuates lipolysis in human adipocytes—a possible link to improved insulin sensitivity. FEBS Lett 582:1725–1730
25. **Izumiya Y, Bina HA, Ouchi N, Akasaki Y, Kharitonenkov A, Walsh K** 2008 FGF21 is an Akt-regulated myokine. FEBS Lett 582:3805–3810